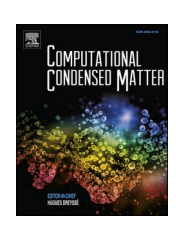
ELSEVIER

Contents lists available at ScienceDirect

Computational Condensed Matter

journal homepage: www.elsevier.com/locate/cocom





Effect of transition metals doping in magnetic properties of Fe₃Se₄

Nabil Al Agtash^{a,*}, Ahmad Alsaad^b, Anas Y. Al-Reyahi^a, Hao Zeng^c, Renat F. Sabirianov^d

- a Department of Physics, Faculty of Science, The Hashemite University, P. O. Box 330127, Zarqa, 13133, Jordan
- ^b Department of Physical Sciences, Jordan University of Science & Technology, P.O. Box 3030, Irbid, 22110, Jordan
- ^c Department of Physics, SUNY, Buffalo, NY, 14260, USA
- ^d University of Nebraska at Omaha, Omaha, NE, 68182, USA

ARTICLE INFO

Keywords: Magnetic properties Monoclinic Fe₃Se₄ TM doping Exchange coupling interaction Magneto crystalline anisotropy

ABSTRACT

We report density functional theory (DFT) study of the magnetic properties of Fe_3Se_4 doped with transition metals, TM (Co, Cr, Ni and Mn), where TM ions are doped in Fe sites to yield $Fe_{2.5}(TM)_{0.5}Se_4$. Screening of the exchange coupling interaction and magnetization modifications were performed upon the substitution of Fe by transition metals at various Fe sites in the Fe_3Se_4 structure. Our study reveals that doping of Fe_3Se_4 with TM elements at Fe sites does not remove antiferromagnetic (AFM) coupling across layers, thus, not increasing the magnetization. This coupling is exhibited by elements with more than half-filled electron shell, i.e. Fe is such an element. Moreover, the exchange coupling between layers of Fe increases strongly as function of interlayer spacing (c lattice parameter) for both pristine and TM-doped Fe_3Se_4 , while the magnetizations of Fe_3Se_4 alloys do not change significantly.

1. Introduction

Fe₃Se₄ has attracted much interest in recent years because of its exciting and unique thermal, electronic, optical, and magnetic properties [1-11]. Crystalline iron selenide (Fe₃Se₄) nanoparticles (NPs) present a valuable model system for a fundamental understanding of apart from having potential applications permanent-magnet-related technologies [11]. Permanent magnets have been employed intensively for the fabrication of a new generation of modern devices. The large market of permanent magnet covers wind turbines, loudspeakers, small rotors, positioning devices in computers, printers, televisions, telephones, and some moving parts of automobiles such as starters, wipers, fan motors, and window regulators. Ferric selenide (Fe₃Se₄) has received re-energized interests in recent years owing to its unique magnetic and electrical properties [12]. These properties make Fe₃Se₄ as a potential candidate for a wide variety of applications in magnetism, spintronics, optoelectronics, thermoelectrics.

Although Fe3Se4 has been studied since the 1950s [13,14], the focus has primarily been on its anisotropy and magnetic structure, with no attempts to increase the energy product by alloying or doping. The bulk crystals of iron selenide with Fe₃Se₄ structure have been characterized, revealing its NiAs-type lattice structure with ordered Fe vacancies [14].

Ferrimagnetic in nature, Fe $_3$ Se $_4$ exhibits a Curie temperature of 314 K, which is above room temperature, and its magneto-crystalline anisotropy is similar to that of permanent magnet materials [15]. The anisotropy can be further enhanced in anisotropic nanostructures, as demonstrated by Fe $_3$ Se $_4$ nanostructures synthesized by Zhang et al. [15] using a simple solution phase method that exhibits hard magnetic properties. At the nanoscale, Fe $_3$ Se $_4$'s ferrimagnetic monoclinic phase has been studied in a few reports [16–19], achieving a coercivity value as large as 40 kOe at 10 K [20]. Change in the magnetic entropy of Fe $_3$ Se $_4$ nanorods in a broad temperature (215–340K) and magnetic field range (0–60 kOe) was studied experimentally by Wang et al. [18]. Magnetic phase transition for Fe $_3$ Se $_4$ has achieved at the Curie temperature T $_c$ ~ 323K [18].

Despite Fe_3Se_4 possesses such a magnetocrystalline anisotropy energy (MAE) and coercivity, the energy product of this compound is small for permanent magnet applications because of its low saturation magnetization. At room temperature, a typical reported magnetization value at a field of 9 T is \sim 5 emu/g [15]; however, smaller values of magnetization, such as 1.89 emu/g at 300 K [18] and 2.2 emu/g at 293 K [17] for Fe_3Se_4 nanostructures, are also reported. Recently, the potential of Fe_3Se_4 as a magnetic energy storage device was investigated. It was found that this compound shows an enormous increase in the energy product while cooling from 300 to 10 K with the potential to replace

E-mail address: nalaqtash76@gmail.com (N. Al Aqtash).

^{*} Corresponding author.

expensive rare-earth hard magnets at lower temperatures [12]. Ghalawat and Poddar find that Fe_3Se_4 is ferrimagnetic below $\sim\!320$ K and show semi-hard magnetic properties [21]. The ferrimagnetism in Fe_3Se_4 arises due to the ordered iron vacancy on the alternate layers of iron [16–19]. Substitution of some Fe with transition metals (TM) ions may have an important influence on the magnetic properties of the system. With the predominant spin polarization on Fe sites, Fe_3Se_4 in its monoclinic phase favors a type-II ferrimagnetic ordering resulting in a total magnetic moment of $\sim\!4.5~\mu\text{B}$ per unit cell. Doping of Fe_3Se_4 potentially may increase magnetization if system converts to ferromagnetic, and/or increase the Curie temperature of the system.

In this work, we reported first principles density functional theory (DFT) study of the magnetic properties of Fe_3Se_4 doped with TM (Co, Cr, Ni and Mn), TM ions doped in Fe sites, $Fe_{2.5}(TM)_{0.5}Se_4$. We performed screening of the exchange coupling interaction and the magnetic moment modifications upon the substitution of Fe with transition metals at various Fe sites in the Fe_3Se_4 structure. The calculations show that the doping of Fe_3Se_4 with TM elements does not remove antiferromagnetic (AFM) coupling across layers. Furthermore, we show a substantial effect of increasing the interlayer spacing (c lattice parameter) on the Curie temperature of the doped Fe_3Se_4 alloys.

2. Computational method

Self-consistent electronic structure calculations were performed for Fe₃Se₄ alloys. The calculations were carried out using the Density-functional theory (DFT) method [22,23] as implemented in the Vienna *ab initio* simulation package VASP [24]. Projector augmented wave PAW pseudopotentials were used [25]. The generalized gradient approximation (GGA) of Perdew-Burke-Ernzerhof (PBE) form [26] is used for the exchange-correlation functional. We used a $9 \times 16 \times 5$ *k*-points sampling for Fe₃Se₄ alloys, the Blöchl's tetrahedron integration method was used [27]. Plane-wave-cut-off energy set to 350 eV and we choose the convergence criteria for energy to be 10^{-6} eV. Calculations were performed with relaxation of atomic positions. We relax the atomic positions of all atoms in the unit cells using Hellmann-Feynman scheme till forces were less than 0.003 eV/Å.

We considered a periodic Fe $_3$ Se $_4$ structure with 6 Fe and 8 Se atoms in the unit-cell. The crystal structure of Fe $_3$ Se $_4$ is a NiAs-type structure, and the Fe vacancies are arranged in an ordered fashion, as shown in Fig. 1. Single crystal studies on Fe $_3$ Se $_4$ have shown that it has a monoclinic unit cell of dimensions a = 6.208 Å, b = 3.525 Å, and c = 11.290 Å [15–17]. We performed a throughput search of the exchange coupling interactions by substituting Fe by 3d-transition metal element that expected to exhibit large local moments such as Co, Cr, Mn, and Ni at various Fe sites in the Fe $_3$ Se $_4$ structure. These Fe $_2$. $_5$ (TM) $_0$. $_5$ Se $_4$ systems were constructed from the unit cell of Fe $_3$ Se $_4$ structure by replacing one Fe atom with TM atom at three different sites, shown in Fig. 1 as I, II &

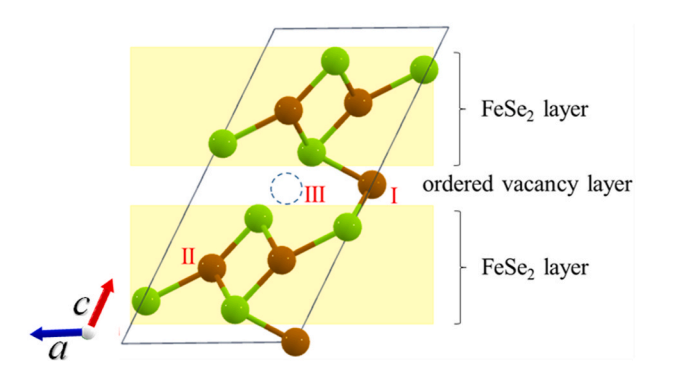


Fig. 1. Unit cell of Fe_3Se_4 and schematic representations of sites doped with TM elements: I - substitutional site within the self-intercalating Fe layer with ordered vacancies, II - substitutional site within $FeSe_2$ layer, and III – ordered vacancy site.

III. All doping cases have the same space group of Fe_3Se_4 structure. Lattice parameters of $Fe_{2.5}$ (TM)_{0.5} Se_4 were fixed at those used for Fe_3Se_4 .

3. Results and discussion

3.1A. Magnetic properties of Fe₃Se₄

The magnetic anisotropy is measured to be 1 MJ/m³ [15], which agrees well with our DFT calculation results. It is unexpected for materials without rare earth or noble metal elements to possess such high anisotropy. Its origin is attributed to the monoclinic structure of Fe₃Se₄ with ordered iron vacancies. The hexagonal symmetry of NiAs-based FeSe crystal structure is dictating the symmetry axis to be along its 6-fold symmetry c-axis. However, vacancies in Fe₃Se₄ order in chains along the b-axis. Alternatively, the system could be represented as layered with FeSe₂ layers separated by "self-intercalating" Fe layer with the vacancies ordered. Such layered structure suggests that magnetocrystalline anisotropy is responsible for the observed large coercivity. The vacancy ordering produces highly anisotropic crystal field and the spin-orbit coupling thus leads to prominent magnetocrystalline anisotropy. To verify this, we performed first-principles calculations of the MAE of Fe₃Se₄. The results of the calculation are presented in Table 1. Our calculation shows that the easy axis is b and the calculated MAE in the order of 1.11 MJ/m³, in agreement with the experimental findings [15]. The magnetic structure of the compound in the ground state is ferrimagnetic, with the calculated difference in energy of the ferromagnetic and ferrimagnetic structures is 0.427 eV/unit cell. The total magnetic moment per unit cell (Fe₆Se₈) is obtained to be 4.5 μ_{R}

3.2. Doping Fe₃Se₄ with transition metals

The large anisotropy of Fe_3Se_4 should be accompanied by large magnetization for permanent magnet applications. The magnetization of Fe_3Se_4 suffers from antiferromagnetic superexchange coupling of Fe across the Se planes. Switching exchange interaction to ferromagnetic would more then double the magnetization. We performed screening of the exchange coupling modifications upon the substitution of Fe by TM (Co, Cr, Mn, and Ni) at various Fe sites in the parent structure. There are three distinct possible sites for doping, i.e. "self-intercalating" site (I), inside $FeSe_2$ layer (II), and vacancy site (III), as shown in Fig. 1.

In order to discuss the effect of the doping on the exchange interactions and the Curie temperature we calculated the difference in energy in FM and AFM magnetic configurations: $\Delta E = E^{AFM} - E^{FM}$. It is analogous (in nearest neighbor approximation) of finding the total onsite Heisenberg exchange parameter in this system $(J_0 = \Delta E/2)$. The Curie temperature is directly proportional to this parameter $(T_c = 2J_0/3k_BT)$, see Table 1.

Table 2 summaries the total magnetic moment and the energy difference between ferromagnetic (FM) and antiferromagnetic (AFM) configurations of spins between neighboring layers of Fe_{2.5}(TM)_{0.5}Se₄ structures. Fig. 2(a) shows the energy difference (Δ E) between FM and AFM configurations of spins between neighboring layers of TMs and the

Table 1
Magnetic properties of Fe₃Se₄ System.

0 1 1	3 7 2		
Property	Theoretical	Experimental Ref. [15]	AlNiCo
Ms(A/m)	0.17×10^{6} (FIM) 0.46×10^{6} (FM)	$0.09\times10^6\text{(FIM)}$	0.9×10^6
K, anisotropy constant	1.11 MJ/m ³	1 MJ/m^3	
(BH) _{max}	8 kJ/m ³ (FIM) 60 kJ/m ³ (FM)	~1 kJ/m ³ (FIM)	10–88 kJ/ m ³
T _c , Curie temperature	420K	320K	850K

Table 2 Total magnetic moment (M) and the exchange interaction analyzed as the energy difference (ΔE) between aligned (FM) and anti-aligned (AFM) configurations of spins between neighboring layers of transition metals (TM) for Fe_{2.5}TM)_{0.5}Se₄. TM positions (I and II) referring to Fig. 1.

Dopant	TM site	M (FM) μ _{B/cell}	$\begin{array}{c} M(AFM) \\ \mu_{B/cell} \end{array}$	E(FM) eV	E(AFM) eV	ΔE eV
Fe ₃ Se ₄		11.16	4.50	-80.7721	-81.1995	0.4274
Co	(I)	10.00	6.59	-79.6831	-79.9796	0.2965
	(II)	10.20	3.71	-79.5242	-79.7679	0.2437
Cr	(I)	12.69	4.17	-82.4694	-82.8287	0.3593
	(II)	12.20	3.60	-82.5454	-82.7268	0.1814
Mn	(I)	11.98	4.14	-81.9771	-82.3717	0.3946
	(II)	12.12	3.14	-82.0050	-82.0607	0.0557
Ni	(I)	9.18	6.06	-78.2721	-78.4833	0.2112
	(II)	9.11	2.83	-78.1455	-78.2583	0.1128

effect of TMs doping in the total magnetic moment (M). The data in Table 2 and Fig. 2(b) show that doping with Co and Ni would increase the magnetization of Fe₃Se₄ if all dopant would occupy the position I. However, with more of the random occupancy, the reduction of magnetization may occur as was experimentally observed [28]. Furthermore, even site I doping may not be that beneficial because it reduces the exchange coupling energy which means reducing Curie temperature (T_c). However, previous work has predicted that the increase in saturation magnetization and T_c were observed in the Cr doping of Fe₃Se₄ crystals [29]. These results reveal that doping of Fe₃Se₄ with TM elements does not remove AFM coupling across layers.

Table 3 shows the magnetocrystalline anisotropy energies (MAE) (MJ/m³) of $Fe_{2.5}(TM)_{0.5}Se_4$ with TM substituting at site I (ordered-vacancy Fe layer). Moreover, data in Table 3 show that doping with TM elements decreases the magnetocrystalline anisotropy energies (MAE) of Fe_3Se_4 .

3.3. C. Effect of interlayer spacing (c parameter)

Meanwhile doping of Fe_3Se_4 with TM elements does not remove AFM coupling across layers. We studied the effect of changing the interlayer spacing (c parameter) of doped structure on the exchange coupling and the magnetization of Fe_3Se_4 structure. We selected Cr doped and Mn doped structures to study the interlayer spacing effect. Fig. 3 shows the energy difference between FM and AFM configurations of spins between neighboring layers of TM and the magnetic moment for $Fe_{2.5}(TM)_{0.5}Se_4$

(at doping position I, Fig. 1) as function interlayer spacing (c parameter).

Fig. 3 indicates that while the magnetic moment of Fe_3Se_4 does not wary significantly as function of strain (as can be seen in the bottom panel), the exchange coupling between layers of Fe increases strongly as function of interlayer spacing (c lattice parameter) for both undoped and TM-doped Fe_3Se_4 (as shown in the top panel). T_c potentially can be increased by 30%. This is reminiscent of the magneto-elastic effects discussed in Fe-based permanent magnets [30]. The magnetoelastic coupling in this case leads the future research to find a dopant that noticeably increase the spacing between $FeSe_2$ layer by doping "self-intercalating" Fe-layer. The dopant elements should be large in size and desirably have propensity for intercalation.

4. Conclusions

Magnetic properties of Fe₃Se₄ doped with TM (Co, Cr, Ni and Mn) were explored as a potential approach to increase the magnetization and Curie temperature of Fe₃Se₄. Density functional theory (DFT) study of the magnetic properties of Fe₃Se₄ doped with TM (Co, Cr, Ni and Mn), TM ions doped in Fe sites, Fe_{2.5}(TM)_{0.5}Se₄ was conducted. Screening of the exchange coupling interaction and the magnetic moment modifications were performed upon the substitution of Fe by TM elements at various Fe sites in the Fe₃Se₄ structure. The study shows that doping Fe₃Se₄ with TM elements does not remove AFM coupling across Fe layers or increase its magnetocrystalline anisotropy energy. However, the increase in the magnetic moment can be obtained for the Co- and Nidoping at Fe sites. The Curie temperature of Fe₃Se₄ alloys may be enlarged by increasing the interlayer spacing (c lattice parameter) due to the strong increase in the exchange coupling between Fe layers. Doping with elements that may intercalate between FeSe2 layers and, therefore, increase the interlayer distances are needed.

Table 3 Magnetocrystalline anisotropy energies (MAE) (MJ/ m^3) of Fe_{2.5}(TM)_{0.5}Se₄ with TM substituting at site I (ordered-vacancy Fe layer).

Alloy\Axis	a	b	c
Fe ₃ Se ₄	0.573	0	1.112
$Fe_{2.5}Co_{0.5}Se_4$	1.006	0	1.111
$Fe_{2.5}Cr_{0.5}Se_4$	0.504	0	0.899
$Fe_{2.5}Mn_{0.5}Se_4$	0.244	0	0.896
$Fe_{2.5}Ni_{0.5}Se_4$	0.158	0	0.764

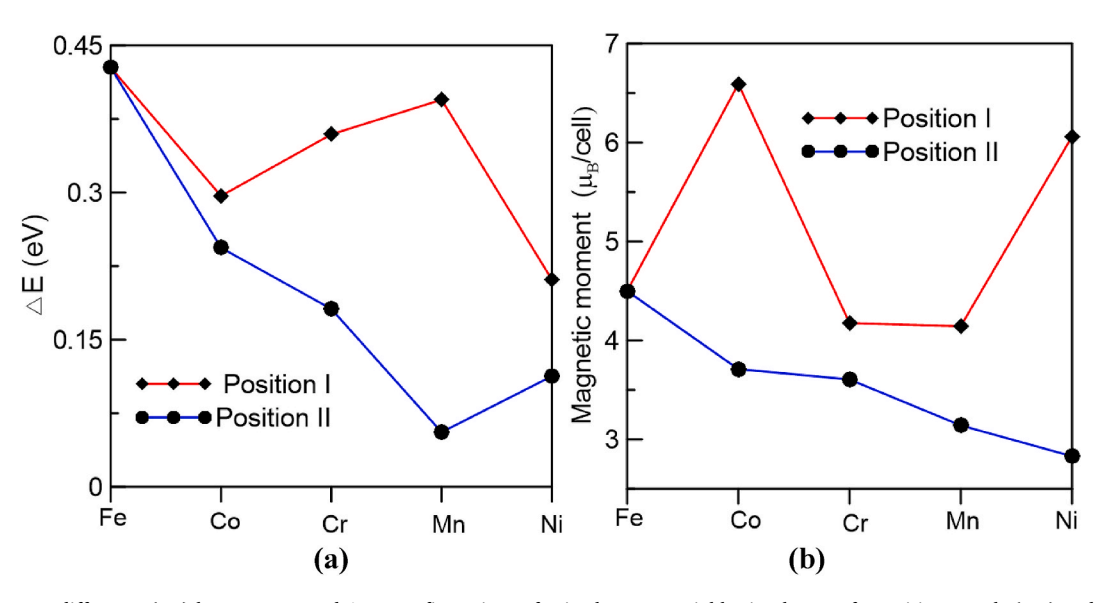


Fig. 2. (a) The energy difference (ΔE) between FM and AFM configurations of spins between neighboring layers of transition metals (TM) and (b) the magnetic moment for Fe_{2.5}(TM)_{0.5}Se₄.

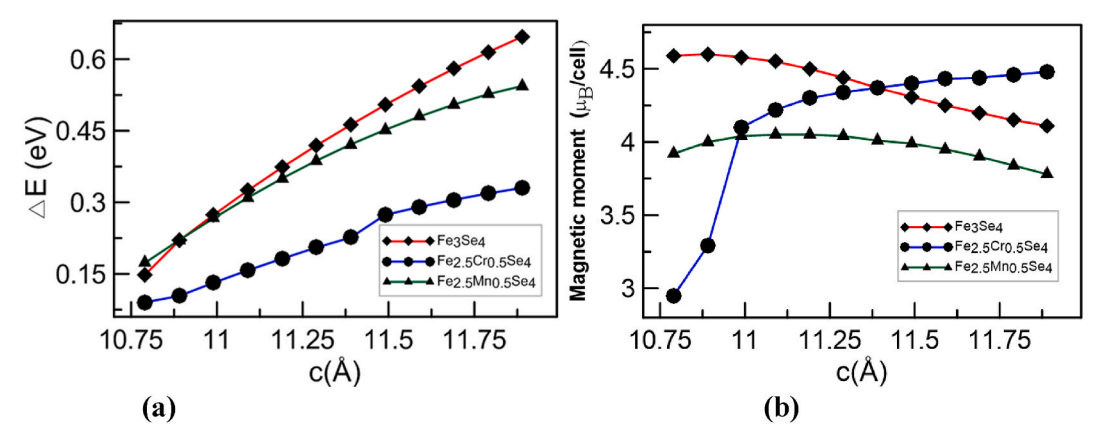


Fig. 3. (a) The energy difference (Δ E) between FM and AFM configurations of spins between neighboring layers of transition metals and (b) the magnetic moment for Fe_{2.5}(TM)_{0.5}Se₄ (at doping position I as function of *c* parameter).

Funding

This research received funding from National Science Foundation, United States; Scientific Research and Innovation Support Fund(award # 2044049) and Scientific Research and Innovation Support Fund, ministry of higher education and scientific research-Jordan and Deanship of Scientific research at JUST (project # 325–2021)

Availability of data

Data associated with this work will be made available upon a reasonable request.

Declaration of competing interest

The authors declare that they have no known competing financial interests or personal relationships that could have appeared to influence the work reported in this paper.

Data availability

Data will be made available on request.

Acknowledgement

The work was supported by National Science Foundation (award # 2044049). This work in parts was supported by Scientific Research and Innovation Support Fund, ministry of higher education and scientific research-Jordan and Deanship of Scientific research at JUST (project # 325–2021). The computations were performed at Holland Computing Center.

References

- P. Santhoshkumar, et al., Hierarchical iron selenide nanoarchitecture as an advanced anode material for high-performance energy storage devices, Electrochim. Acta 356 (Oct. 2020), 136833, https://doi.org/10.1016/j. electacta.2020.136833.
- [2] W. Sun, Y. Li, S. Liu, C. Liu, X. Tan, K. Xie, Mechanism investigation of iron selenide as polysulfide mediator for long-life lithium-sulfur batteries, Chem. Eng. J. 416 (Jul. 2021), 129166. https://doi.org/10.1016/j.cej.2021.129166.
- [3] F. Zhao, et al., Improved sodium-ion storage performance of ultrasmall iron selenide nanoparticles, Nano Lett. 17 (7) (Jul. 2017) 4137–4142, https://doi.org/ 10.1021/acs.nanolett.7b00915.
- [4] B. Pandit, et al., Combined electrochemical and DFT investigations of iron selenide: a mechanically bendable solid-state symmetric supercapacitor, Sustain. Energy Fuels 5 (19) (2021) 5001–5012, https://doi.org/10.1039/D1SE00074H.
- [5] H. Fan, et al., 1D to 3D hierarchical iron selenide hollow nanocubes assembled from FeSe2@C core-shell nanorods for advanced sodium ion batteries, Energy Storage Mater. 10 (Jan. 2018) 48–55, https://doi.org/10.1016/j. ensm.2017.08.006.

- [6] S. Thanikaikarasan, R. Perumal, S. Roji Marjorie, Influence of potential on structural, compositional, optical and magnetic properties of electrochemically grown iron selenide thin films, J. Alloys Compd. 848 (Dec. 2020), 156348, https:// doi.org/10.1016/j.jallcom.2020.156348.
- [7] D. Guterding, H.O. Jeschke, R. Valentí, Basic electronic properties of iron selenide under variation of structural parameters, Phys. Rev. B 96 (12) (Sep. 2017), 125107, https://doi.org/10.1103/PhysRevB.96.125107.
- [8] J.P. Rodriguez, Spin resonances in iron selenide high-Tc superconductors by proximity to a hidden spin density wave, Phys. Rev. B 102 (2) (Jul. 2020), 024521, https://doi.org/10.1103/PhysRevB.102.024521.
- [9] S. Lu, et al., Iron selenide microcapsules as universal conversion-typed anodes for alkali metal-ion batteries, Small 17 (8) (Feb. 2021), 2005745, https://doi.org/ 10.1002/smll.202005745
- [10] K.F. Ulbrich, C.E.M. Campos, Stability of iron selenide nanophases prepared by mechanosynthesis, AIP Adv. 9 (4) (Apr. 2019), 045311, https://doi.org/10.1063/ 1.5084262
- [11] M. Ghalawat, P. Poddar, Study of growth kinetics of Fe ₃ Se ₄ nanocrystallites and the influence of size and shape tunability on their magnetic properties, J. Phys. Chem. C 125 (14) (Apr. 2021) 7932–7943, https://doi.org/10.1021/acs. ipcc 1.00389
- [12] M. Sen Bishwas, R. Das, P. Poddar, Large increase in the energy product of Fe 3 Se 4 by Fe-site doping, J. Phys. Chem. C 118 (8) (Feb. 2014) 4016–4022, https://doi.org/10.1021/jp411956q.
- [13] A.F. Andresen, E. Vestersjø, A. Haaland, S. Gronowitz, H. Christiansen, U. Rosén, A neutron diffraction investigation of Fe3Se4, Acta Chem. Scand. 22 (1968) 827–835, https://doi.org/10.3891/acta.chem.scand.22-0827.
- [14] K. Hirakawa, The magnetic properties of iron selenide single crystals, J Physical Soc Japan 12 (8) (Aug. 1957) 929–938, https://doi.org/10.1143/JPSJ.12.929.
- [15] H. Zhang, G. Long, D. Li, R. Sabirianov, H. Zeng, Fe ₃ Se ₄ nanostructures with giant coercivity synthesized by solution chemistry, Chem. Mater. 23 (16) (Aug. 2011) 3769–3774. https://doi.org/10.1021/cm/201610k.
- [16] Chun-Rong Lin, Yu-Jhan Siao, Shin-Zong Lu, Chie Gau, Magnetic properties of iron selenide nanocrystals synthesized by the thermal decomposition, IEEE Trans. Magn. 45 (10) (Oct. 2009) 4275–4278, https://doi.org/10.1109/ TMAG 2009 2025256
- [17] G. Long, H. Zhang, D. Li, R. Sabirianov, Z. Zhang, H. Zeng, Magnetic anisotropy and coercivity of Fe ₃ Se ₄ nanostructures, Appl. Phys. Lett. 99 (20) (Nov. 2011), 202103. https://doi.org/10.1063/1.3662388.
- [18] J. Wang, H. Duan, X. Lin, V. Aguilar, A. Mosqueda, G. Zhao, Temperature dependence of magnetic anisotropy constant in iron chalcogenide Fe ₃ Se ₄: excellent agreement with theories, J. Appl. Phys. 112 (10) (Nov. 2012), 103905, https://doi.org/10.1063/j.4759359
- [19] D. Li, J.J. Jiang, W. Liu, Z.D. Zhang, Positive magnetoresistance in Fe ₃ Se ₄ nanowires, J. Appl. Phys. 109 (7) (Apr. 2011), 07C705, https://doi.org/10.1063/1.3544508
- [20] M.J. Kramer, R.W. McCallum, I.A. Anderson, S. Constantinides, Prospects for nonrare earth permanent magnets for traction motors and generators, JOM 64 (7) (Jul. 2012) 752–763, https://doi.org/10.1007/s11837-012-0351-z.
- [21] M. Ghalawat, P. Poddar, Remarkable effect of Fe and Se composition on magnetic Properties—Comparative study of the Fe–Se system at the nanoscale, J. Phys. Chem. C 126 (9) (Mar. 2022) 4655–4663, https://doi.org/10.1021/acs.jpcc.1c10286.
- [22] P. Hohenberg, W. Kohn, Inhomogeneous electron gas, Phys. Rev. 136 (3B) (Nov. 1964) B864–B871, https://doi.org/10.1103/PhysRev.136.B864.
- [23] W. Kohn, L.J. Sham, Self-consistent equations including exchange and correlation effects, Phys. Rev. 140 (4A) (Nov. 1965) A1133–A1138, https://doi.org/10.1103/ PhysRev.140.A1133.
- [24] G. Kresse, D. Joubert, From ultrasoft pseudopotentials to the projector augmentedwave method, Phys. Rev. B 59 (3) (Jan. 1999) 1758–1775, https://doi.org/ 10.1103/PhysRevB.59.1758.
- [25] P.E. Blöchl, Projector augmented-wave method, Phys. Rev. B 50 (24) (Dec. 1994) 17953–17979, https://doi.org/10.1103/PhysRevB.50.17953.

- [26] J.P. Perdew, K. Burke, M. Ernzerhof, Generalized gradient approximation made simple, Phys. Rev. Lett. 77 (18) (Oct. 1996) 3865–3868, https://doi.org/10.1103/ PhysRevLett 77 3865
- [27] P.E. Blöchl, O. Jepsen, O.K. Andersen, Improved tetrahedron method for Brillouin-zone integrations, Phys. Rev. B 49 (23) (Jun. 1994) 16223–16233, https://doi.org/10.1103/PhysRevB.49.16223.
- [28] H. Zhang, G. Long, D. Li, R. Sabirianov, H. Zeng, Fe3Se4 nanostructures with giant coercivity synthesized by solution chemistry, Chem. Mater. 23 (16) (2011) 3769–3774, https://doi.org/10.1021/cm201610k.
- [29] D. Li, S. J. Li, B. J. Dong, T. Yang, W. Liu, and Z. D. Zhang, "Large magnetocrystalline anisotropy of Fe_{3-x}Cr_xSe₄ single crystals due to Cr substitution," Europhys. Lett., Vol. 109, no. 3, pp. 37004, DOI 10.1209/0295-5075/109/37004.
- [30] R.F. Sabirianov, S.S. Jaswal, Electronic structure and magnetism in Sm2Fe17-xAx (A=Al,Ga,Si), J. Appl. Phys. 79 (1996) 5942, https://doi.org/10.1063/1.362114.